Kinase fusion positive intra-osseous spindle cell tumors

Suurmeijer, Albert J H; Xu, Bin; Torrence, Dianne; Dickson, Brendan C; Antonescu, Cristina R

Published in:
Genes Chromosomes & Cancer

DOI:
10.1002/gcc.23205

Publication date:
2024

Received: 20 July 2023 | Revised: 18 September 2023 | Accepted: 21 September 2023

DOI: 10.1002/gcc.23205

RESEARCH ARTICLE

WILEY

Kinase fusion positive intra-osseous spindle cell tumors: A series of eight cases with review of the literature

Albert J. H. Suurmeijer[1] | Bin Xu[2] | Dianne Torrence[3] | Brendan C. Dickson[4] | Cristina R. Antonescu[2]

[1]Department of Pathology, University Medical Center Groningen, University of Groningen, Groningen, The Netherlands

[2]Department of Pathology, Memorial Sloan Kettering Cancer Center, New York, New York, USA

[3]Department of Pathology, Northwell Health (Long Island Jewish Medical Center), New Hyde Park, New York, USA

[4]Department of Pathology & Laboratory Medicine, Mount Sinai Hospital, Toronto, Canada

Correspondence
Cristina R. Antonescu, Memorial Sloan Kettering Cancer Center, 1275 York Ave, New York, NY 10021, USA.
Email: antonesc@mskcc.org

Funding information
Kristin Ann Carr Foundation, Grant/Award Numbers: P30 CA008748, P50 CA217694

Abstract

Mesenchymal spindle cell tumors with kinase fusions, often presenting in superficial or deep soft tissue locations, may rarely occur in bone. Herein, we describe the clinicopathologic and molecular data of eight bone tumors characterized by various kinase fusions from our files and incorporate the findings with the previously reported seven cases, mainly as single case reports. In the current series all but one of the patients were young children or teenagers, with an age range from newborn to 59 years (mean 19 years). Most tumors ($n = 5$) presented in the head and neck area (skull base, mastoid, maxilla, and mandible), and remaining three in the tibia, pelvic bone, and chest wall. The fusions included *NTRK1* ($n = 3$), *RET* ($n = 2$), *NTRK3* ($n = 2$), and *BRAF* ($n = 1$). In the combined series ($n = 15$), most tumors (73%) occurred in children and young adults (<30 years) and showed a predilection for jaw and skull bones (40%), followed by long and small tubular bones (33%). The fusions spanned a large spectrum of kinase genes, including in descending order *NTRK3* ($n = 6$), *NTRK1* ($n = 4$), *RET* ($n = 2$), *BRAF* ($n = 2$), and *RAF1* ($n = 1$). All fusions confirmed by targeted RNA sequencing were in-frame and retained the kinase domain within the fusion oncoprotein. Similar to the soft tissue counterparts, most *NTRK3*-positive bone tumors in this series showed high-grade morphology (5/6), whereas the majority of *NTRK1* tumors were low-grade (3/4). Notably, all four tumors presenting in the elderly were high-grade spindle cell sarcomas, with adult fibrosarcoma (FS)-like, malignant peripheral nerve sheath tumor (MPNST)-like and MPNST phenotypes. Overall, 10 tumors had high-grade morphology, ranging from infantile and adult-types FS, MPNST-like, and MPNST, whereas five showed benign/low-grade histology (MPNST-like and myxoma-like). Immunohistochemically (IHC), S100 and CD34 positivity was noted in 57% and 50%, respectively, while co-expression of S100 and CD34 in 43% of cases. One-third of tumors (4 high grade and the myxoma-like) were negative for both S100 and CD34. IHC for Pan-TRK was positive in all eight *NTRK*-fusion positive tumors tested and negative in two tumors with other kinase fusions. Clinical follow-up was too limited to allow general conclusions.

KEYWORDS
bone, fibrosarcoma, fusion, malignant peripheral nerve sheath tumor, NTRK, RET, sarcoma

1 | INTRODUCTION

About 20 years after the initial description in 1998 of the canonical *ETV6::NTRK3* fusion in infantile fibrosarcoma (IFS),[1] and with the advent of next generation sequencing (NGS), other gain-of-function kinase fusions have been reported in subsets of soft tissue and bone tumors, spanning various clinical presentations, histologic types, and risk of malignancy.[2] Apart from the *NTRK1*-rearranged lipofibromatosis-like neural tumor (LPFNT),[3] this emerging tumor family also includes a heterogeneous group of rare but distinct spindle cell tumors with *NTRK1-3*, *RAF1*, *BRAF*, *ALK*, and *RET* fusions, often displaying a malignant peripheral nerve sheath tumor (MPNST) or fibrosarcoma (FS)-like phenotype and associated with immunohistochemical co-expression of S100 and CD34.[4–6] This group of neoplasms encompasses low-grade tumors composed of a monomorphic spindle cell proliferation with haphazard growth, often with distinctive patterns of keloidal stromal and perivascular collagen deposition, as well as intermediate to high-grade tumors composed of cellular solid and fascicular areas of monomorphic spindle cells with hyperchromatic nuclei, scant cytoplasm, and increased mitotic rate. More recently, this family of kinase fusion positive spindle cell tumors has been divided into several subcategories mainly based on morphologic features and immunohistochemical (IHC) profiles, to reflect their similarities with other established soft tissue tumors and allow a more readily pattern-recognition by practicing pathologists. These include: LPFNT reminiscent of a lipofibromatosis, infantile fibrosarcoma (IFS)-like in patients younger than 2 years of age and exclusive of the canonical *ETV6::NTRK3* fusion, adult type FS-like, MPNST-like, and myxoma-like (see Table 1).[7] Notwithstanding, these tumors also appear to be part of a continuous morphologic spectrum as several cases showed hybrid or overlapping histologic features, for example, lipofibromatosis-like patterns alternating with solid areas of cellular fascicular growth or tumors displaying both low-grade and high-grade morphology.[8] However, these descriptive morphologic designations have been proven effective in pre-selecting tumors that may require further PanNTRK IHC staining or molecular sequencing. Members of this rare family of mesenchymal tumors with kinase fusions may occur in different anatomic sites, including skin, superficial and deep soft tissue, bone, gynecologic tract, and gastrointestinal tract.[9–12] Herein, we present eight primary bone tumors with kinase fusions (BTKF), the largest series to date, and compare our findings to seven other case reports in the recent literature.

TABLE 1 Phenotypic subcategories of kinase gene associated mesenchymal spindle cell tumors (modified from Xu et al.[7]).

IFS	S100-negative primitive (blue) spindle cell tumor, often with fascicular/herringbone arrangement, occurring in patients below age of 2 years old, harboring the canonical *ETV6::NTRK3* fusion
IFS-like	IFS phenotype as defined above, with alternative kinase fusions other than *ETV6::NTRK3*
LPFNT	Tumor with monotonous bland spindle cells showing a highly infiltrative pattern within adjacent adipose tissue at the periphery, frequent co-expression of S100 and CD34, prominent bands of stromal collagen, and perivascular hyalinization
MPNST-like	S100-positive cellular spindle cell tumor showing exclusive solid architecture, frequent stromal collagen deposits, and perivascular hyalinization
Adult FS-like	S100-negative cellular spindle cell tumor showing exclusive solid architecture, often with fascicular/herringbone arrangement, occurring in patients ≥2 y
Myxoma-like	Hypocellular hypovascular myxoid neoplasm with bland stellate to spindle cells

2 | MATERIALS AND METHODS

2.1 | Patient selection and clinicopathologic review

Candidate cases were retrieved from the pathology archives of MSKCC and UMCG and the personal consultation cases of two of the authors (A.J.H.S. and C.R.A.) based on the presence of kinase gene fusion or rearrangement as documented by molecular studies (fluorescence in situ hybridization [FISH] or targeted RNA sequencing). All identified bone tumors with kinase fusions included in this study were reviewed by two pathologists (A.J.H.S. and C.R.A.) to gather relevant histopathologic parameters, demographic, and outcome data. Five of the eight tumors have been previously reported, as shown in Table 2. IMT cases with typical morphology and *ALK* or *ROS1* fusions were excluded from the study. Each tumor was further subdivided into IFS, IFS-like tumor, LPFNT, MPNST-like, adult FS-like, and myxoma-like based on their histologic features, immunoprofile, and underlying fusion using earlier definitions provided by Xu et al. (Table 1). Immunohistochemistry studies were reviewed for the following primary antibodies: S100 (polyclonal, dilution: 1:8000, DAKO; Agilent), CD34 (clone: QBEnd-10, ready to use [RTU], Ventana; Roche Diagnostics), and pan-TRK (clone EPR17341, dilution 1:100; Abcam). Staining was performed on a Leica-Bond-3 (Leica, Buffalo Grove, IL) or a Ventana Benchmark (Ventana Medical Systems, Tucson, AZ) automated immunostaining platform using a heat-based antigen retrieval method and high pH buffer.

2.2 | Targeted RNA sequencing and FISH detection of kinase fusions

2.2.1 | Targeted RNA sequencing

For the Illumina MiSeq platform (used in three cases), RNA was extracted from formalin-fixed paraffin embedded (FFPE) tissue using Amsbio's ExpressArt FFPE Clear RNA Ready kit (Amsbio LLC, Cambridge, MA). All cases had adequate RNA quality and could be further processed and analyzed. RNA-seq libraries were prepared using 20–100 ng total RNA with the TruSight RNA Fusion Panel (Illumina, San Diego, CA). Targeted RNA sequencing was performed

TABLE 2 Clinicopathological, molecular, and outcome data of eight bone tumors with kinase fusions.

Case	Age/Sex	Location	Kinase Gene	Partner	Size (cm)	Histology	MI	Atypia	S100	CD34	pan-NTRK	FU (months)
1[a]	Newborn/M	Skull base	NTRK3	ETV6	4.7	IFS	3	N	Neg	Neg	Pos	NA
2[b]	2 mo/M	Chest wall	RET	CLIP2	NA	IFS-like	5	NA	Neg	Neg	NA	NED (114)
3[c]	4 y/M	Mandible	NTRK1	LMNA	4	LG-MPNST-like	5	N	Pos	Pos	Pos	NED (142)
4[c]	13 y/M	Maxilla	NTRK1	LMNA	2.5	LG-MPNST-like	0	N	Pos	Pos	Pos	NED (648)
5	9 y/F	Pelvis/ilium	NTRK1	TPM3	8.7	HG-MPNST-like	>20	N	Pos	Neg	Pos	Recent case
6	14 y/M	Mastoid	BRAF	FNBP1	NA	HG-adult FS-like	>10	N: necrotic	Neg	Neg	NA	Recent case
7	59 y/F	Tibia	NTRK3	UPF2	5.6	HG-MPNST	>10	Y	Neg	Neg	Pos	NA
8[a]	15 y/M	Skull base	RET	KIF5B	1.3	Myxoma-like	0	N	Neg	Neg	Neg	NA

Abbreviations: F, female; M, male; N, no; NA, not available; neg, negative; pos, positive.
[a]Xu et al.[7]
[b]Antonescu et al.[6]
[c]Suurmeijer et al.[4]

on an Illumina MiSeq platform, as previously described.[4] Reads were independently aligned with STAR (version 2.3) against the human reference genome (hg19) and analyzed by STAR-Fusion. The detailed procedure for the two cases studied by the Archer Anchored Multiplex RNA sequencing assay has also been previously described.[13] In short, unidirectional gene-specific primers were designed to target specific exons in 62 genes known to be involved in oncogenic fusions in solid tumors. RNA was extracted from FFPE specimens, followed by cDNA synthesis and library preparation. Anchored Multiplex polymerase chain reaction amplicons were sequenced on Illumina Miseq, and the data was analyzed using the Archer software. In one case the commercially available FoundationOneHeme comprehensive genomic profiling test was applied. This assay combines DNA and RNA sequencing, among others for the sensitive detection of known and novel fusions in sarcomas using FFPE material. In this case the novel finding of *UPF2::NTRK3* was confirmed by running a RNA-based NGS panel from a second lab (NeoGenomics sarcoma comprehensive fusion panel).

2.2.2 | Fluorescence in situ hybridization

Two cases were tested by FISH for gene abnormalities relevant to that particular case (both detecting *LMNA::NTRK1*). Custom probes made by bacterial artificial chromosomes (BAC) clones flanking the genes of interest (*LMNA*, *NTRK1*) as previously described,[3] according to UCSC genome browser (http://genome.ucsc.edu) and obtained from BACPAC sources of Children's Hospital of Oakland Research Institute (Oakland, CA; http://bacpac.chori.org). DNA from each BAC was isolated according to the manufacturer's instructions. The BAC clones were labeled with fluorochromes (fluorescent-labeled dUTPs, Enzo Life Sciences, New York, NY) by nick translation and validated on normal metaphase chromosomes. The 4 μm thick FFPE slides were deparaffinized, pretreated, and hybridized with denatured probes, as previously described.[4] After overnight incubation, the slides were washed, stained with 4′,6-diamidino-2-phenylindole, mounted with an antifade solution, and then examined on a Zeiss1 fluorescence microscope (Zeiss Axioplan, Oberkochen, Germany) controlled by Isis 5 software (Metasystems).

3 | RESULTS

A total of eight bone tumors with confirmed kinase fusions were selected from our files. The clinicopathological features, IHC profile, underlying fusion events, and clinical outcome are summarized in Table 2.

3.1 | Clinical features

All except one of the patients in the current cohort were young children or teenagers. The patient age ranged from newborn (congenital IFS case) to 59 years (mean 19 years, median 11 years). By location, most tumors ($n = 5$) presented in the head and neck area (skull base ($n = 2$), mastoid, maxilla, and mandible), but few also occurred in tibia, pelvic bone, and chest wall, involving one of the ribs. Data on imaging studies were available in three cases (case #1, case #5, and case #7), while in the remaining the skeletal location was confirmed by radiologic reports and/or gross appearance within the bone. Case #1 concerned a maxillary tumor which by CT scans revealed a well-demarcated and lytic expansile tumor with invasion of surrounding soft tissue (Figure 1A). Case #5 was a pelvic bone tumor originating in the iliac wing, in which the MRI scans showed a 13-month interval size increase, from $4.6 \times 2.3 \times 4.4$ cm to $8.7 \times 6.4 \times 5.4$ cm. The tumor characteristics were that of a well-defined lytic lesion with cortical breakthrough and soft tissue extension with invasion of the iliopsoas muscle. In case #7, plain X-ray and MRI scans showed a $5.6 \times 2.8 \times 2.5$ cm infiltrative destructive lesion in the proximal tibia with cortical breakthrough, extending in surrounding soft tissue, and abutting the neurovascular bundle (Figure 2A).

3.2 | Molecular findings

In the current cohort, the kinase genes affected were *NTRK1* ($n = 3$), *RET* ($n = 2$), *NTRK3* ($n = 2$), and *BRAF* ($n = 1$). Kinase fusions were detected by RNA sequencing methods in six cases showing in-frame

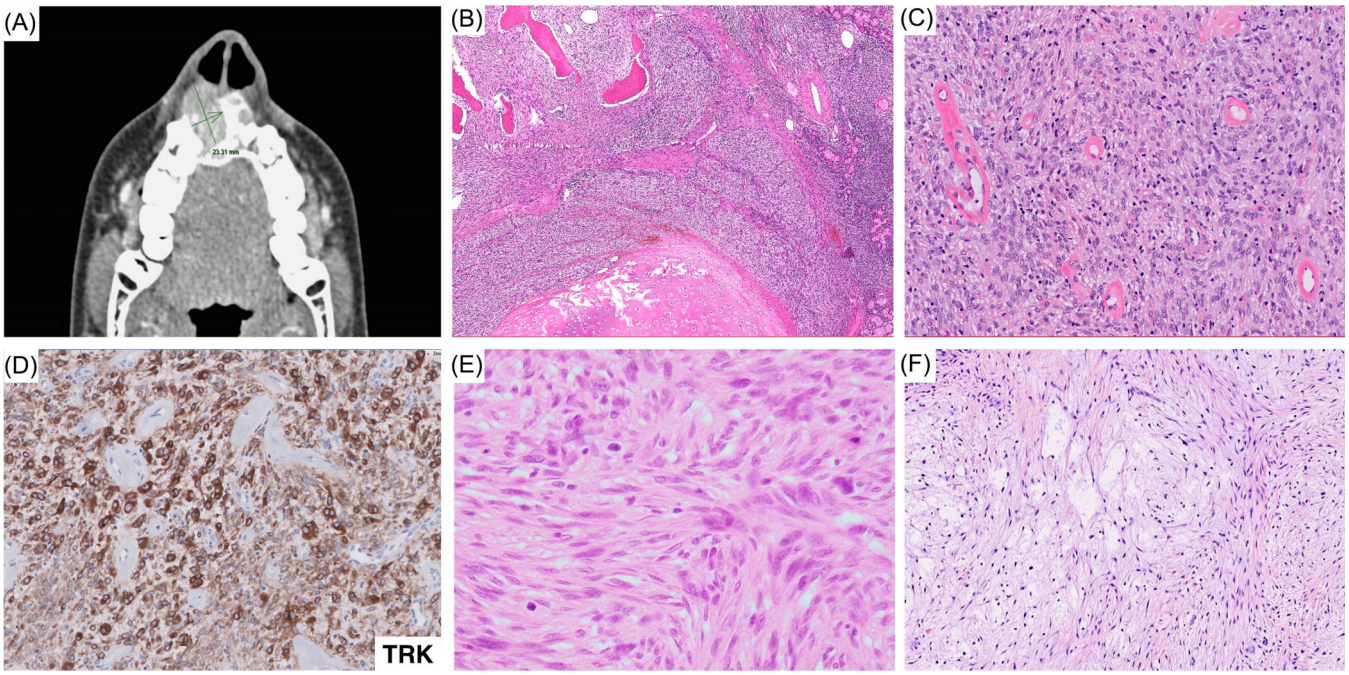

FIGURE 1 BTKF (bone tumor with kinase fusion) with low-grade MPNST-like and myxoma-like morphology. (A–E) A 2.5 cm LG-MPNST-like lesion with *LMNA::NTRK1* fusion (case #4) involving maxilla showing aggressive clinical features with CT imaging including cortical breakthrough and soft tissue extension (A). This tumor is composed of vague fascicles of bland spindle cells infiltrating bone and cartilage (B). At higher power the tumor shows haphazardly arranged uniform spindle cells, dense keloid-like stromal changes and marked perivascular hyalinization (C). The tumor is positive for Pan-TRK (D). (E) Mandible tumor representing a LG-MPNST-like tumor with *LMNA::NTRK1* fusion (case #3) showing fascicles of uniform eosinophilic myofibroblast-like spindle cells. (F) Myxoma-like histology: skull base tumor with *KIF5B::RET* fusion (case #8). This hypocellular and hypovascular tumor is composed of bland stellate cells in an abundant myxoid background and indistinguishable from myxoma of bone.

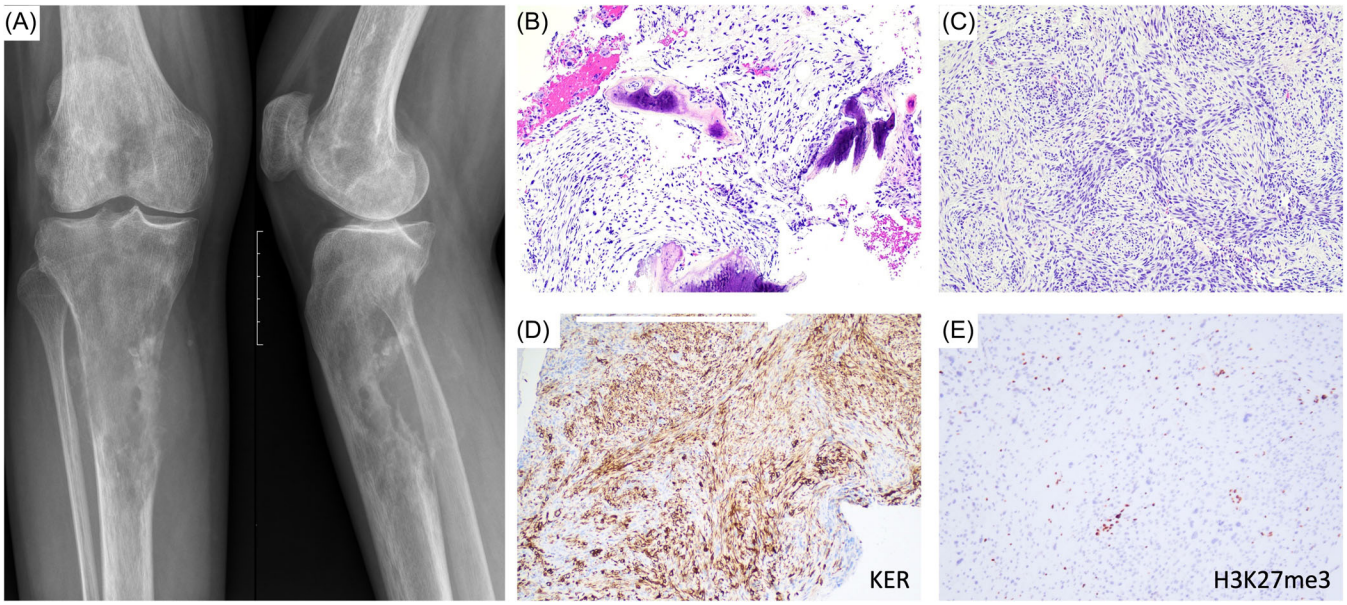

FIGURE 2 Primary MPNST of bone with *UPF2::NTRK3* fusion, occurring in the proximal tibia of a-29-year-old female. Plain radiograph shows an ill-defined destructive bone tumor with cortical breakthrough and soft tissue extension (A). The tumor is composed of perpendicular fascicles of monomorphic hyperchromatic (blue) spindle cells (B–C), which show expression of cytokeratin (D) and loss of trimethylated histone protein H3K27 (E).

gene products including the kinase domain. The transcript gene fusions were between *ETV6* exon 5 and *NTRK3* exon 15 ($n = 1$, case #1); between *CLIP2* exon 14 and *RET* exon 12 (case #2); between *TPM3* exon 7 and *NTRK1* exon 10 (case #5); between *FNBP1* exon 10 and *BRAF* exon 9 (case #6); between *KIF5B* exon 5 and *RET* exon 15 (case #8), and between *UPF2* exon 3 and *NTRK3* exon 4 (case

#7). In case #7, representing a primary MPNST of bone, additional molecular findings included: *P53* H179L mutation, loss of *CDKN2A*, and loss of *EED*. The remaining two cases were confirmed to have a *LMNA::NTRK1* fusion by FISH (case #3 and case #4).

3.3 | Histologic features and IHC profile

All bone lesions were subclassified based on their histologic features and IHC profile into distinctive morphologic phenotypes, as defined in Table 1 and presented in Table 2, including classic IFS ($n = 1$), IFS-like ($n = 1$), adult FS-like ($n = 1$), low-grade and high-grade MPNST-like tumor ($n = 3$), and myxoma-like tumor ($n = 1$). In addition, one case represented a primary MPNST arising in bone. The histologic features were diverse. The three MPNST-like tumors appeared to correlate with *NTRK1* fusions. In addition to the malignant phenotype displayed by the IFS and IFS-like tumor, there were three other tumors that showed features in keeping with a high-grade sarcoma, based on nuclear atypia, elevated mitotic index of ≥10 per 10 HPFs, and tumor necrosis, including one MPNST-like tumor with *TPM3::NTRK1* (case #5), one adult FS-like tumor with *FNBP1::BRAF* fusion (case #6), and one MPNST with *UPF2::NTRK3* fusion (case #7).

3.4 | Infantile fibrosarcoma and infantile fibrosarcoma-like

There were two bone tumors in this cohort which had a FS phenotype and occurred in infants. One congenital skull base tumor harbored the canonical *ETV6::NTRK3* fusion (case #1) was designated as classic IFS albeit with unusual morphologic features, while another chest wall tumor presenting in a 2-months-old newborn male showed the presence of a *CLIP2::RET* fusion and was considered a molecular variant of IFS (or IFS-like, case #2). Histologically, case #1 revealed a cystic lesion surrounded by a thick fibrous capsule with mural nodules showing cystic hemorrhagic change, and solid growth with an HPC-like vascular pattern, and heavy lymphocytic infiltrate (Figure 3A–C). Case #2 showed hypercellular solid growth with spindle cells arranged in intersecting fascicles with the prototypical herringbone pattern or as sheets of ovoid cells forming ill-formed fascicles (Figure 3E, F). Mitotic index ranged from 3 to 5 mitotic figures (MFs) per 10 HPFs. None of the IFSs showed perivascular hyalinization, dense hyalinized collagen bands, or areas reminiscent of lipofibromatosis. IHC staining for Pan-TRK was performed in IFS with *ETV6::NTRK3* fusion (case #1) which showed heterogeneous cytoplasmic immunopositivity (Figure 3D). Both tumors (IFS and IFS-like) were negative for S100 and CD34.

3.5 | MPNST-like tumors and MPNST

In three MPNST-like cases (cases #3–5), the tumor had a solid growth and showed features resembling MPNST, composed of primitive uniform blue ovoid to spindle cells with scant cytoplasm arranged haphazardly or in a vague fascicular or angiopericytic pattern (Figure 1B, C, E). Perivascular hyalinization and stromal collagen bands were prominent in case #3 (Figure 1C). In this subset, two tumors (case #3 and case #5) had low-grade morphology, whereas an iliac bone

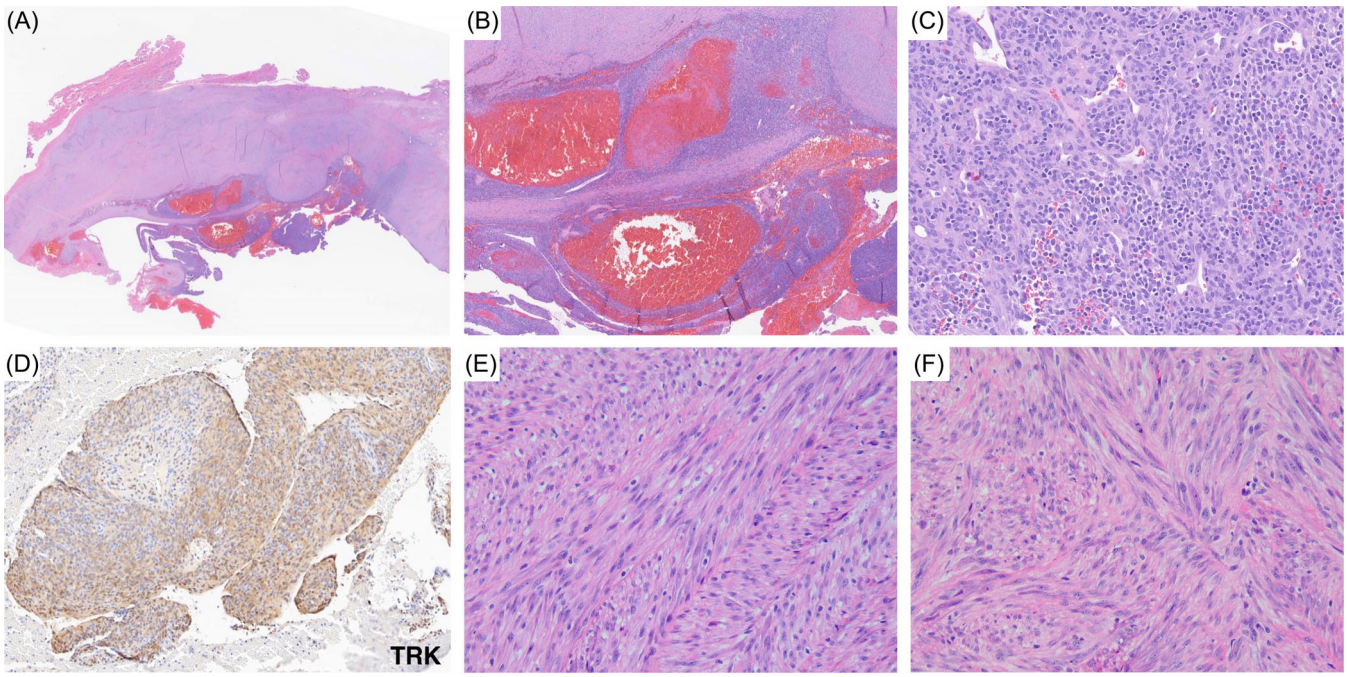

FIGURE 3 BTKF showing high-grade FS-like patterns. (A–D) IFS with *ETV6::NTRK3* fusion (case #1) composed of a cystic lesion surrounded by a thick fibrous capsule with mural nodules (A) showing cystic hemorrhagic change (B) and solid growth with HPC-like vascular pattern and heavy lymphocytic infiltrate (C), and IHC staining for Pan-TRK (D). (E-F) IFS-like tumor with *CLIP2::RET* fusion (case #2) composed of fascicles of spindle cells in herringbone (E) and intersecting patterns (F).

tumor harboring *TPM3*::*NTRK1* in a 9-year-old patient (case #4) showed high-grade features with a mitotic index exceeding 20/10 HPFs, but no tumor necrosis. All three MPNST-like tumors were positive for S100. CD34 immunopositivity was seen in case #3 and case #5 but was absent in case #4. IHC for Pan-TRK showed diffuse cytoplasmic staining in all three cases, including *LMNA*::*NTRK1* ($n = 2$), and *TPM3*::*NTRK1*, respectively (Figure 1D). Case #7 represented a unique case of a primary MPNST of bone with an *UPF2*::*NTRK3* fusion, occurring in the proximal tibia of a 59-year-old female. This high-grade MPNST showed mitotically active monotonous blue spindle cells invading bone and arranged in a fascicular and perpendicular pattern. The diagnosis of MPNST was further confirmed by the NGS report showing in addition to the *NTRK3* fusion, the presence of *CDKN2A/B* loss, *TP53 H179L* mutation and *EED* loss. The tumor showed an overall low mutational burden (0 mutations/Mb) and was microsatellite stable. Based on this genomic landscape, IHC was performed to investigate alterations of the PRC2 complex, showing complete loss of H3K27me3 in the tumor cells, further support for the diagnosis of MPNST. Additionally, tumor cells were positive for pan-cytokeratin and Pan-TRK (Figure 2B–E).

3.6 | Adult-type FS

Case #6 was a mastoid bone tumor presenting in a 14-year-old male patient, which harbored a *FNBP1*::*BRAF* fusion. Tumor histology was high grade with nuclear atypia, high mitotic index of >10 mitoses in 10 HPF, and extensive tumor necrosis. CD34 and S100 were negative in this tumor.

3.7 | Unusual histotype of myxoma-like tumor

Case #8, a skull base tumor arising in a 15-year-old boy, showed an unusual hypocellular, hypovascular myxoid appearance indistinguishable from myxoma of bone (Figure 1F). The tumor was composed entirely of bland stellate and spindle cells in a myxoid background. There was no mitotic activity, cytologic atypia, or tumor necrosis. The initial histologic differential diagnosis of this case was intraosseous myxoma or fibrous dysplasia. IHC was negative for S100, CD34, and Pan-TRK. Targeted RNA sequencing revealed a *KIF5B*::*RET* fusion.

3.8 | Pan-TRK immunostaining

IHC staining for Pan-TRK, performed in 6/7 cases, was positive with cytoplasmic staining in all five cases with *NTRK1/3* fusion (Figures 1D and 3D) and negative in the case with *RET* fusion. No nuclear immunopositivity was seen in this cohort.

3.9 | Clinical outcome

Clinical follow-up was limited as most of them represented consultation cases. Clinical outcome was only available in three cases with a follow-up period of 114 to 648 months (median: 142 months). The three cases included the IFS-like tumor with *CLIP2*::*RET* presenting in the chest wall of a 2-month-old baby boy and both low-grade MPNST-like tumors with *LMNA*::*NTRK1* occurring in the maxilla and mandible. These three patients showed no evidence of disease; none of them developed recurrences or metastatic disease after major surgery. Two other cases were recent diagnoses.

4 | DISCUSSION

In the past decade, next generation sequencing technology has significantly contributed to refining the classification of soft tissue and bone tumors enabling the detection of genomic alterations in a single step.[14] This has resulted, among others, in the discovery of several novel gene fusions that are associated with distinct but until then unrecognized tumor types. A good example of this development are kinase fusions detected across mesenchymal tumors with uniform spindle cell morphology.

In 2016, *NTRK1* fusions were first described to define lipofibromatosis-like neural tumors (LPFNT), a monomorphic spindle cell neoplasm with keloidal and perivascular collagen deposition, infiltrating subcutaneous fat in a reticular fashion and often showing IHC co-expression of S100 and CD34.[3] Notably, LPFNT lacks SOX10 expression, which distinguish them from other histologic look-alikes, such as lipofibromatosis or nerve sheath tumors. LPFNT has not been associated with history of NF1 and behaves in a benign fashion, with only local recurrences being described if incompletely excised. Anecdotal evidence, based on rare patients with large inoperable tumors with this phenotype showed dramatic clinical responses to kinase inhibitor therapy and became resectable, albeit with positive margins (Antonescu, Suurmeijer personal communication, and Baranov et al.).[15] Although initially described as a distinct pathologic entity mostly harboring *NTRK1* fusions, it was subsequently recognized that LPFNT may present as a focal component within a tumor with hybrid LPFNT and solid patterns, and can harbor other kinase fusions, including *NTRK2/3*, *RET*, *ALK*, and *MET*. The outcome of patients with tumors with hybrid histology remains mostly benign, with only one isolated case with a low-grade histology in a series of 24 patients developing distant metastatic disease to the lung.[8]

Another phenotype commonly associated with kinase fusions represents a more heterogeneous group of spindle cell tumors that frequently co-express S100 and CD34 and resemble low-grade MPNSTs.[4] These lesions belong to an emerging family of rare mesenchymal spindle cell tumors showing a wide morphologic spectrum and clinical behavior, harboring not only *NTRK* rearrangements, but also *RAF1*, *BRAF*, or *RET* fusions. Most of these tumors (60%) occur in the superficial or deep soft tissues of the extremities and trunk of children or young adults (<30 years old) of both genders.

Finally, a subgroup of FS-like or MPNST-like tumors represent higher grade lesions, which have a predilection for *NTRK3* gene fusions.[5] On very rare occasions, these tumors are associated with neurofibromatosis (NF1).[16] Clinical follow-up, albeit limited, has emphasized

that tumors with a high-grade malignant phenotype have the propensity for distant spread and follow an aggressive clinical course.[4,5]

Some of the detected *NTRK3*, *RET*, and *BRAF* kinase fusions in this series were novel or uncommon. Notably, in all of these fusion variants, the predicted chimeric amino acid sequence was in-frame and contained the kinase activation domain. Therefore, these kinase fusions likely represent oncogenic drivers. In case #7 representing a prototypical MPNST of bone, a previously unreported *UPF2*::*NTRK3* fusion was detected by two different RNA sequencing platforms (Illumina TruSight and Neogenomics). The notion that this rare occurrence of an *NTRK3* fusion in MPNST represents a driver event is supported by a recent case report of a sciatic nerve MPNST with another novel *SNRNP70*::*NTRK3* fusion. In this case, the tumor showed a fast and durable response to the NTRK inhibitor entrectinib for 10 months.[17] The *KIF5B*::*RET* fusion found in a single myxoma-like tumor (case #8) has also been reported as a molecular event in an adult FS-like tumor arising in the small intestine.[18] In addition, this gene fusion represents a common driver alteration in non-small cell lung cancer.[19] Although the *FNBP1*::*BRAF* fusion detected in an adult FS-like tumor (case #6) has only been reported in a single case of a primary lung melanoma,[20] several cases of *BRAF*-rearranged spindle cell neoplasms with many other fusion partners and IFS-like or FS-like morphology have been published in the literature.[21,22]

To date (including eight cases from the current study), 15 patients with mesenchymal spindle cell tumors originating from bone and harboring kinase fusions were reported in the literature after excluding prototypical cases of IMT.[4,6,7,15,23–26] The clinicopathologic features, fusion events, and IHC profile of these cases are summarized in Table 3. Four tumors presenting in children below the age of 2 years were classified by default as IFS/IFS-like tumors. Most of the other cases (7/11) occurred in children and young adults (< 30 years). This propensity for teenagers and young adults is also reported for mesenchymal neoplasms with kinase fusions from other body sites.[7] Notably, all four tumors seen in the elderly were high-grade FS-like, MPNST-like tumors or MPNST. By location, bone tumors with kinase fusions (BTKF) had a variable anatomic distribution, often presenting in jaw and skull bones (6/15; 40%) and long and small tubular bones (5/15; 33%), and less commonly in pelvic bones (2/15), vertebrae (1/15), and ribs (1/15). By imaging studies (radiographs, computed tomography, MRI), available in three cases, lesions appeared well-demarcated, lytic tumors with aggressive features such as cortical destruction and invasion in surrounding soft tissue. Akin to mesenchymal neoplasms from other body sites the most frequently rearranged kinase genes were *NTRK3* ($n = 6$) and *NTRK1* ($n = 4$), whereas those involving *RET* ($n = 2$), *BRAF* ($n = 2$), and *RAF1* ($n = 1$) were less common. BTKF cases displayed a wide morphologic spectrum and were further subdivided in six phenotypic groups, based on age at presentation, histology, and S100 protein expression, as first described by Xu et al.[7] Overall, 10 (67%) tumors had high-grade morphology (IFS, IFS-like, adult FS like, HG MPNST-like, and MPNST), whereas five (33%) cases were low-grade (LG MPNST-like and myxoma-like). Similar to soft tissue locations, most *NTRK3* bone tumors in this series showed high-grade morphology (5/6), whereas the majority of *NTRK1* tumors were low-grade (3/4). By reported IHC findings, S100 and CD34 positivity was noted in 57% and 50%, respectively. The immunoprofiles of BTKF varied according to histologic subcategories. Notably, 5 (33%)

TABLE 3 Fusion events, clinicopathological and outcome data of 15 bone tumors with kinase fusion genes combining our cases with those retrieved from the literature.

Case	Reference	Age/sex	Location	Kinase gene	Fusion partner	Size (cm)	Histology	MI	Atypia	S100	CD34	Pan-TRK	Outcome
1	#16	Newborn/F	Lumbosacral	NTRK3	ETV6	5	IFS	1	N	Pos	Pos	Pos	NA
2	#17	Newborn/M	Sphenoid	NTRK3	ETV6	NA	IFS	NA	N	NA	NA	NA	NA
3	#7	Newborn/M	Skull base	NTRK3	ETV6	4.7	IFS	3	N	Neg	Neg	Pos	NA
4	#6	2 mo/M	Chest wall	RET	CLIP2	NA	IFS-like	5	NA	Neg	Neg	NA	NED (114)
5	#4	4 y/M	Mandible	NTRK1	LMNA	4	LG-MPNST-like	5	N	Pos	Pos	Pos	NED (142)
6	#16	12 y/M	Pelvis	NTRK1	TPM3	9.9	LG-MPNST-like	1	N	Pos	Pos	Pos	NA
7	#18	21 y/F	Femur	NTRK3	HMBOX1	>5	LG-MPNST-like	0	N	Pos	Neg	Pos	NA
8	#4	13 y/M	Maxilla	NTRK1	LMNA	2.5	LG-MPNST-like	0	N	Pos	Pos	Pos	NED (648)
9	#19	60 y/F	Femur	RAF1	MAP4	9.7	HG-MPNST-like	12	N	Pos	Pos	Neg	NA
10	#20	73 y/F	Metacarpal	BRAF	KIAA1549	4.9	HG-MPNST-like	4	Focal atypia	Pos	Pos	NA	NA
11	#21	38 y/F	Radius	NTRK3	STRN	8.7	Adult FS-like	3	N	Neg	Pos	NA	AWD (113)
12	#7	15 y/M	Skull base	RET	KIF5B	1.3	Myxoma-like	0	N	Neg	Neg	Neg	NA
13	Recent case	9 y/F	Pelvis/ilium	NTRK1	TPM3	8.7	HG-MPNST-like	>20	N	Pos	Neg	Pos	Recent case
14	Recent case	14 y/M	Mastoid	BRAF	FNBP1	NA	HG-adult FS-like	>10	N: necrotic	Neg	Neg	NA	Recent case
15	Recent case	59 y/F	Tibia	NTRK3	UPF2	5.6	HG-MPNST	>10	Y	Neg	Neg	Pos	Recent case

Abbreviations: AWD, alive with disease; F, female; M, male; N, no; NA, not available; NED, no evidence of disease; neg, negative; pos, positive.

tumors (4 high grade and one myxoma-like) were negative for both S100 and CD34. Pan-TRK was seen in all eight *NTRK*-fusion positive tumors tested but was negative in two tumors with other kinase fusions. Importantly, as was shown in a recent Dutch nationwide analysis of 69 cases including different cancer types, overall, IHC for Pan-TRK has limited sensitivity (around 80%) for *NTRK1-3* fusion genes.[27] For this reason, although Pan-TRK immunohistochemistry may be used as a screening tool for tumors with possible *NTRK* fusion genes, molecular tests are required if there is high suspicion based on histologic features (resembling FS or MPNST) and immunoprofiles (CD34 and/or S100). Given the wide variety of gene fusions encountered in these tumors, targeted RNA sequencing is preferred. In this cohort, clinical follow-up was too limited to allow any general conclusions. With respect to the whole group of mesenchymal tumors with kinase gene fusions, studies with larger cohorts would increase our understanding of prognostic factors that determine differences in outcome between low-grade and high-grade morphology, superficial and deep tumor localization, occurrence in children or adult patients, and gene fusion type. To date, the number of such studies is very limited. Historically, classic IFS with *ETV6::NTRK3* is considered to be a locally aggressive and rarely metastasizing tumor.[28] Notably, in a small series of childhood tumors, no statistical difference was seen in any clinicopathologic feature between the classic IFS with *ETV6::NTRK3* and other pediatric *NTRK*-rearranged mesenchymal tumors.[29] In contrast, in a meta-analysis of 46 *NTRK*-rearranged uterine sarcomas, several adverse prognostic features were established, including a mitotic index ≥8 per 10 HPF, lymphovascular invasion, necrosis, and *NTRK3* fusion. Patients with uterine tumors lacking any of these four features had an excellent prognosis.[30] Although patients with BTKF may be eligible for tyrosine kinase inhibitor therapy,[31] none of the patients in this series received such treatment, as most of these older diagnoses preceded the availability of tyrosine kinase inhibitors in clinical use.

Given their rarity and variable clinicopathologic features in terms of age at presentation, bone location and uniform spindle cell morphology, the differential diagnosis of BTKF is broad and challenging. Primary spindle cell tumors of bone (without kinase gene fusions) entering the differential diagnosis includes both fibrous, osteoblastic, and neural neoplasms. Moreover, as primary bone occurrence of some of these tumor entities all are exceptionally rare, the clinical possibility of metastatic manifestations should be ruled out. In the jaw and skull bones, myxoma-like BTKF must be differentiated from myxoma of jaw bones and (myxoid) fibrous dysplasia.

Solitary fibrous tumor (SFT) of bone may strongly resemble low-grade MPNST-like BTKF as these entities represent monomorphic spindle cell tumors with haphazard growth, stromal collagen, perivascular hyalinization, hemangiopericytoma-like vessels, and expression of CD34.[32] However, SFT may be differentiated by STAT6 IHC expression or demonstration of the characteristic *NAB2::STAT6* fusion. Fibroblastic osteosarcoma may occasionally display a pure/predominantly spindle cell proliferation, but in a larger sample focal osteoid deposition and multifocal IHC expression of SATB2 can be detected. Other extremely rare skeletal presentations of soft tissue tumors, such as the monophasic variant of synovial sarcoma and classic MPNST, may be confused with high-grade variants of FS-like or MPNST-like BTKF.[33–36] Although neurofibromatosis (NF1)-association is common in classic MPNST, rare cases of high-grade MPNST-like kinase fusion tumors have been reported recently to occur in the setting of NF1.[16] However, in contrast to BTKF, classic MPNST often shows loss of the H3K27me3 expression,[37] as shown in the unique case #7 included in this series, which represents a primary MPNST of bone and harboring *UPF2::NTRK3* fusion in addition to *TP53* H179L mutation, loss of *CDKN2A/B*, and loss of *EED*. The patient did not have clinical history or stigmata of NF1. It is tempting to speculate that the *NTRK3* fusion detected in this case represents a late, acquired event in an otherwise phenotypically and genomically typical case of a high grade MPNST. This is further supported by the fact that most if not all *NTRK*-fusion positive high grade spindle cell neoplasms tested in our experience retain the H3K27me3 expression, which is lost in most high grade MPNST regardless of NF1 status.[37]

Myxoma of jaw bones and myxoma-like BTKF can only be differentiated by molecular studies, demonstrating the presence of a kinase fusion gene in the latter.[7] Myxoid variants of fibrous dysplasia occurring in jaw or skull bones may sometimes lack areas with typical metaplastic ossification (irregular trabeculae of woven bone without rimming of mature osteoblasts) but can be diagnosed by *GNAS* mutation analysis.[38]

In conclusion, we reviewed and evaluated 15 BTKF, including eight cases from our files. These tumors showed highly variable age at presentation and anatomic site distribution. Most tumors were seen in teenagers and young adults. Jaw and skull bones and long tubular bones were most commonly affected. Akin to mesenchymal tumors with kinase fusions in soft tissue locations, *NTRK1* and *NTRK3* were the most common fusion events, all of which were demonstrable by IHC for Pan-TRK in this series. Other fusion genes included *RET*, *BRAF*, and *RAF1*. Given the wide variety of possible gene rearrangements in BTKF, a targeted RNA sequencing technique is preferred for diagnostic purposes and selecting patients that are eligible for kinase inhibitor therapy.

FUNDING INFORMATION

Supported in part by: P50 CA217694 (CRA), P30 CA008748, Cycle for Survival (CRA), Kristin Ann Carr Foundation (CRA).

DATA AVAILABILITY STATEMENT

Upon reasonable request we can provide additional information on the reported cases. however, no repository is established as no raw NGS data is available.

ORCID

Albert J. H. Suurmeijer https://orcid.org/0000-0003-1361-9454
Bin Xu https://orcid.org/0000-0003-4638-9835
Brendan C. Dickson https://orcid.org/0000-0003-2269-6216
Cristina R. Antonescu https://orcid.org/0000-0002-9717-8205

REFERENCES

1. Knezevich SR, McFadden DE, Tao W, Lim JF, Sorensen PH. A novel ETV6-NTRK3 gene fusion in congenital fibrosarcoma. *Nat Genet*. 1998;18(2):184-187.

2. Antonescu CR. Emerging soft tissue tumors with kinase fusions: an overview of the recent literature with an emphasis on diagnostic criteria. *Genes Chromosomes Cancer*. 2020;59(8):437-444.
3. Agaram NP, Zhang L, Sung YS, et al. Recurrent NTRK1 gene fusions define a novel subset of locally aggressive lipofibromatosis-like neural tumors. *Am J Surg Pathol*. 2016;40(10):1407-1416.
4. Suurmeijer AJH, Dickson BC, Swanson D, et al. A novel group of spindle cell tumors defined by S100 and CD34 co-expression shows recurrent fusions involving RAF1, BRAF, and NTRK1/2 genes. *Genes Chromosomes Cancer*. 2018;57(12):611-621.
5. Suurmeijer AJ, Dickson BC, Swanson D, et al. The histologic spectrum of soft tissue spindle cell tumors with NTRK3 gene rearrangements. *Genes Chromosomes Cancer*. 2019;58(11):739-746.
6. Antonescu CR, Dickson BC, Swanson D, et al. Spindle cell tumors with RET gene fusions exhibit a morphologic spectrum akin to tumors with NTRK gene fusions. *Am J Surg Pathol*. 2019;43(10):1384-1391.
7. Xu B, Suurmeijer AJH, Agaram NP, Antonescu CR. Head and neck mesenchymal tumors with kinase fusions: a report of 15 cases with emphasis on wide anatomic distribution and diverse histologic appearance. *Am J Surg Pathol*. 2023;47(2):248-258.
8. Kao YC, Suurmeijer AJH, Argani P, et al. Soft tissue tumors characterized by a wide spectrum of kinase fusions share a lipofibromatosis-like neural tumor pattern. *Genes Chromosomes Cancer*. 2020;59(10):575-583.
9. Llamas-Velasco M, Itlinger-Monshi B, Flucke U, Mentzel T. Dermal lipofibromatosis-like neural tumor. *J Cutan Pathol*. 2022;49(6):525-531.
10. Surrey LF, Davis JL. NTRK-rearranged soft tissue neoplasms: a review of evolving diagnostic entities and algorithmic detection methods. *Cancer Genet*. 2022;260-261:6-13.
11. Chiang S, Cotzia P, Hyman DM, et al. NTRK fusions define a novel uterine sarcoma subtype with features of fibrosarcoma. *Am J Surg Pathol*. 2018;42(6):791-798.
12. Atiq MA, Davis JL, Hornick JL, et al. Mesenchymal tumors of the gastrointestinal tract with NTRK rearrangements: a clinicopathological, immunophenotypic, and molecular study of eight cases, emphasizing their distinction from gastrointestinal stromal tumor (GIST). *Mod Pathol*. 2021;34(1):95-103.
13. Zheng Z, Liebers M, Zhelyazkova B, et al. Anchored multiplex PCR for targeted next-generation sequencing. *Nat Med*. 2014;20(12):1479-1484.
14. Nacev BA, Sanchez-Vega F, Smith SA, et al. Clinical sequencing of soft tissue and bone sarcomas delineates diverse genomic landscapes and potential therapeutic targets. *Nat Commun*. 2022;13(1):3405.
15. Baranov E, Winsnes K, O'Brien M, et al. Histologic characterization of paediatric mesenchymal neoplasms treated with kinase-targeted therapy. *Histopathology*. 2022;81(2):215-227.
16. Hiemcke-Jiwa LS, Meister MT, Martin E, et al. NTRK rearrangements in a subset of NF1-related malignant peripheral nerve sheath tumors as novel actionable target. *Acta Neuropathol*. 2023;145(1):149-152.
17. Kobayashi H, Makise N, Shinozaki-Ushiku A, et al. Dramatic response to entrectinib in a patient with malignant peripheral nerve sheath tumor harboring novel SNRNP70-NTRK3 fusion gene. *Genes Chromosomes Cancer*. 2023;62(1):47-51.
18. Zhao M, Yin X, He H, Xia Q, Ru G. Recurrent RET fusions in fibrosarcoma-like neoplasms in adult viscera: expanding the clinicopatological and genetic spectrum. *Histopathology*. 2023;82(3):633-645.
19. Nagasaka M, Brazel D, Baca Y, et al. Pan-tumor survey of RET fusions as detected by next-generation RNA sequencing identified RET fusion positive colorectal carcinoma as a unique molecular subset. *Transl Oncol*. 2023;36:101744.
20. Kervarrec T, Jean-Jacques B, Pissaloux D, Tirode F, de la Fouchardiere A. FNBP1-BRAF fusion in a primary melanoma of the lung. *Pathology*. 2021;53(6):785-788.
21. Kao YC, Fletcher CDM, Alaggio R, et al. Recurrent BRAF gene fusions in a subset of pediatric spindle cell sarcomas: expanding the genetic Spectrum of tumors with overlapping features with infantile fibrosarcoma. *Am J Surg Pathol*. 2018;42(1):28-38.
22. Penning AJ, Al-Ibraheemi A, Michal M, et al. Novel BRAF gene fusions and activating point mutations in spindle cell sarcomas with histologic overlap with infantile fibrosarcoma. *Mod Pathol*. 2021;34(8):1530-1540.
23. Steelman C, Katzenstein H, Parham D, et al. Unusual presentation of congenital infantile fibrosarcoma in seven infants with molecular-genetic analysis. *Fetal Pediatr Pathol*. 2011;30(5):329-337.
24. Wang Z, Wang J. Primary NTRK-rearranged spindle cell neoplasm of bone harboring an HMBOX1::NTRK3 gene fusion. *Genes Chromosomes Cancer*. 2023;62(8):477-482.
25. Yeung MCF, Lam AYL, Shek TWH. Novel MAP4::RAF1 fusion in a primary bone sarcoma: expanding the spectrum of RAF1 fusion sarcoma. *Int J Surg Pathol*. 2022;30(6):682-688.
26. Yamazaki F, Nakatani F, Asano N, et al. Novel NTRK3 fusions in fibrosarcomas of adults. *Am J Surg Pathol*. 2019;43(4):523-530.
27. Koopman B, Kuijpers C, Groen HJM, et al. Detection of NTRK fusions and TRK expression and performance of pan-TRK immunohistochemistry in routine diagnostics: results from a Nationwide Community-based cohort. *Diagnostics (Basel)*. 2022;12(3):668.
28. Chung EB, Enzinger FM. Infantile fibrosarcoma. *Cancer*. 1976;38(2):729-739.
29. Davis JL, Lockwood CM, Stohr B, et al. Expanding the spectrum of pediatric NTRK-rearranged mesenchymal tumors. *Am J Surg Pathol*. 2019;43(4):435-445.
30. Costigan DC, Nucci MR, Dickson BC, et al. NTRK-rearranged uterine sarcomas: clinicopathologic features of 15 cases, literature review, and risk stratification. *Am J Surg Pathol*. 2022;46(10):1415-1429.
31. Laetsch TW, DuBois SG, Mascarenhas L, et al. Larotrectinib for paediatric solid tumours harbouring NTRK gene fusions: phase 1 results from a multicentre, open-label, phase 1/2 study. *Lancet Oncol*. 2018;19(5):705-714.
32. Verbeke SL, Fletcher CD, Alberghini M, et al. A reappraisal of hemangiopericytoma of bone; analysis of cases reclassified as synovial sarcoma and solitary fibrous tumor of bone. *Am J Surg Pathol*. 2010;34(6):777-783.
33. Sbaraglia M, Righi A, Gambarotti M, Vanel D, Picci P, Dei Tos AP. Soft tissue tumors rarely presenting primary in bone: diagnostic pitfalls. *Surg Pathol Clin*. 2017;10(3):705-730.
34. Righi A, Gambarotti M, Benini S, et al. Primary synovial sarcoma of bone: a retrospective analysis of 25 patients. *Histopathology*. 2022;80(4):686-697.
35. Gambarotti M, Righi A, Sbaraglia M, et al. Primary malignant peripheral nerve sheath tumors of bone: a clinicopathologic reappraisal of 8 cases. *Hum Pathol*. 2022;122:92-102.
36. Antonescu CR, Erlandson RA, Huvos AG. Primary leiomyosarcoma of bone: a clinicopathologic, immunohistochemical, and ultrastructural study of 33 patients and a literature review. *Am J Surg Pathol*. 1997;21(11):1281-1294.
37. Prieto-Granada CN, Wiesner T, Messina JL, Jungbluth AA, Chi P, Antonescu CR. Loss of H3K27me3 expression is a highly sensitive marker for sporadic and radiation-induced MPNST. *Am J Surg Pathol*. 2015;40:479-489.
38. Pereira T, Gomes CC, Brennan PA, Fonseca FP, Gomez RS. Fibrous dysplasia of the jaws: integrating molecular pathogenesis with clinical, radiological, and histopathological features. *J Oral Pathol Med*. 2019;48(1):3-9.

How to cite this article: Suurmeijer AJH, Xu B, Torrence D, Dickson BC, Antonescu CR. Kinase fusion positive intraosseous spindle cell tumors: A series of eight cases with review of the literature. *Genes Chromosomes Cancer*. 2024;63(1):e23205. doi:10.1002/gcc.23205